Eur. Phys. J. C (2022) 82:164
https://doi.org/10.1140/epjc/s10052-022-10113-6

THE EUROPEAN PHYSICAL JOURNAL C

Regular Article - Theoretical Physics

Lepton universality and lepton flavor conservation tests with dineutrino modes

Rigo Bause[a], **Hector Gisbert**[b], **Marcel Golz**[c], **Gudrun Hiller**[d]

Fakultät für Physik, TU Dortmund, Otto-Hahn-Str. 4, 44221 Dortmund, Germany

Received: 19 November 2021 / Accepted: 7 February 2022 / Published online: 22 February 2022

Abstract $SU(2)_L$-invariance links charged dilepton and dineutrino couplings. Phenomenological implications are worked out for flavor changing neutral currents involving strange, charm, beauty and top quark transitions in a model-independent way. We put forward novel tests of lepton universality and lepton flavor conservation in $|\Delta c| = |\Delta u| = 1$ and $|\Delta b| = |\Delta q| = 1$, $q = d, s$, transitions suitable for the experiments Belle II and BES III. Single top production plus dileptons uniquely probes semileptonic four-fermion $|\Delta t| = |\Delta q'| = 1$, $q' = u, c$, couplings and further study at the LHC is encouraged. Tests with single top production associated with dileptons and missing energy are suitable for study at future e^+e^- or muon colliders.

1 Introduction

Gauge and approximate flavor symmetries of the standard model (SM) provide powerful means to probe new physics (NP). In this work we exploit the $SU(2)_L$-link between left-handed charged lepton and neutrino couplings, to put quantitatively lepton universality (LU) and charged lepton flavor conservation (cLFC) to the test with dineutrino observables. Schematically,

$$\begin{aligned} O(\nu\bar{\nu}) &= \sum_{i,j} O(\nu_i \bar{\nu}_j) = \sum_{i,j} O(\ell_i^- \ell_j^+) \\ &= O(e^-e^+) + O(\mu^-\mu^+) + O(\tau^-\tau^+) \\ &\quad + O(e^-\tau^+) + \ldots \end{aligned}$$

where we used that the neutrino flavors i, j are not reconstructed and the ellipses stand for the remaining charged lepton flavor violating (cLFV) terms. Apparently observables $O(\nu\bar{\nu})$ can be bounded by a sum of lepton-flavor specific data. Assuming cLFC, only same-flavor charged dilepton observables contribute. Assuming in addition universality, the strongest limit among the dielectron, dimuon and ditau observables dictates the bound. Confronting data on dineutrino observables to charged dilepton ones hence probes lepton flavor.

Somewhat paradoxically, the method works despite the fact that in dineutrino observables lepton flavor is not determined. The method is independent of the neutrino mixing matrix and holds for NP contributions from above the weak scale. The relation works of course also the other way around: dineutrino limits bounding charged dilepton couplings [1]. In the end it is a matter of available data which direction is informative on BSM physics. Given the huge improvements over the past years this analysis is timely. With the flavor anomalies challenging LU [2,3] such quantitative data-driven tests of lepton flavor are important and of recent interest.

We consider observables involving quark flavor changing neutral currents (FCNCs) and dineutrinos, but note that the method works analogously for flavor conserving quark transitions. We furthermore employ the standard model effective theory (SMEFT), which provides a model-independent parametrization of NP in terms of higher dimensional operators composed out of SM degrees of freedom and which respect SM gauge and Lorentz invariance. SM gauge symmetry also dictates a relation between the weak isospin partners of the left-handed $SU(2)_L$ doublet quarks. The situation is very different for FCNC processes involving up-type quarks and down-type quarks due to a strong Glashow-Iliopoulos-Maiani (GIM)-suppression of SM amplitudes in the former [4,5], together with weaker experimental constraints, compared to the latter. As such, rare kaon and b-decay data constrain charm and top FCNCs, respectively, and not the other way around. The other important consequence of the GIM-mechanism is that signals of up-type dineutrino FCNCs

[a] e-mail: rigo.bause@tu-dortmund.de
[b] e-mail: hector.gisbert@tu-dortmund.de (corresponding author)
[c] e-mail: marcel.golz@tu-dortmund.de
[d] e-mail: ghiller@physik.uni-dortmund.de

are automatically signals of NP. It is a central point of this work that, once observed, the rate at which these missing energy processes occur is informative on the violation of LU and cLFC, complementing tests with lepton-specific ratio-$\mathcal{O}(\mu^+\mu^-)/\mathcal{O}(e^+e^-)$ a la R_K [2].

The aim of this work is twofold: firstly, to present a global perspective of LU and cLFC tests using dineutrino couplings in quark FCNCs, by discussing jointly different flavor sectors, strange, charm, beauty and top. Secondly, we work out implications from rare kaon decays and investigate opportunities with top FCNCs to probe for universality violation and beyond.

While the connection between lepton flavor violation and dineutrino branching ratios has been discussed for kaons [6] and B-decays, e.g. [7] and references therein, the actual relation we obtain, (2), and its use in concrete tests of lepton flavor universality is new.

The paper is organized as follows: in Sect. 2 we give the effective theory framework and general relations between neutrino and charged lepton couplings. We analyze NP implications for first and second generation quarks, strangeness and charm, in Sect. 3, and for processes involving third generation quarks in Sect. 4. In Sect. 5 we summarize.

2 Model-independent relation and lepton flavor

Consider the $SU(3)_C \times SU(2)_L \times U(1)_Y$-invariant effective theory with semileptonic (axial-) vector four-fermion operators induced by NP at a scale sufficiently separated from the weak scale $v = (\sqrt{2}\,G_F)^{-1/2} \simeq 246\,\text{GeV}$ at lowest order [8], with Wilson coefficients $C_{\ell q}^{(1)}$, $C_{\ell q}^{(3)}$, $C_{\ell u}$, $C_{\ell d}$,

$$\begin{aligned}\mathcal{L}_{\text{eff}} \supset\ & \frac{C_{\ell q}^{(1)}}{v^2}\bar{Q}\gamma_\mu Q\,\bar{L}\gamma^\mu L + \frac{C_{\ell q}^{(3)}}{v^2}\bar{Q}\gamma_\mu\tau^a Q\,\bar{L}\gamma^\mu\tau^a L \\ & + \frac{C_{\ell u}}{v^2}\bar{U}\gamma_\mu U\,\bar{L}\gamma^\mu L + \frac{C_{\ell d}}{v^2}\bar{D}\gamma_\mu D\,\bar{L}\gamma^\mu L\,.\end{aligned} \tag{1}$$

Here, τ^a are Pauli-matrices, Q and L denote left-handed quark and lepton $SU(2)_L$-doublets and U, D stand for right-handed up-singlet, down-singlet quarks, respectively, with flavor indices suppressed for brevity. No further dimension six four-fermion operators exist that contribute at lowest order to dineutrino modes assuming only SM-like light neutrinos. Operators with dimension larger than six contribute at least with relative suppression by two orders of the ratio of weak to NP scales. Operators with quarks or leptons with two Higgs fields Φ and a covariant derivative D^μ, $\bar{Q}\gamma_\mu Q\,\Phi^\dagger D^\mu\Phi$, $\bar{Q}\gamma_\mu\tau^a Q\,\Phi^\dagger D^\mu\tau^a\Phi$, $\bar{U}\gamma_\mu U\,\Phi^\dagger D^\mu\Phi$, $\bar{D}\gamma_\mu D\,\Phi^\dagger D^\mu\Phi$ and $\bar{L}\gamma_\mu L\,\Phi^\dagger D^\mu\Phi$, $\bar{L}\gamma_\mu\tau^a L\,\Phi^\dagger D^\mu\tau^a\Phi$ induce Z-penguins at tree level, see Fig. 1, – the lepton ones conserve quark flavor, the quark ones obey LU, mixed ones are of higher order in $\mathcal{L}_{\text{eff}}$. These operators are constrained by electroweak and top observables, or mixing [9,10] and are negligible for the purpose of this work. Therefore, the (axial-)vector operators (1), which are invariant under QCD-evolution [11], provide a model-independent basis for the description of dineutrino modes. Effects from electroweak renormalization group running [12] can be neglected for the precision aimed at with this study, since they represent a correction of less than 5% for $\Lambda_{\text{NP}} \sim 10\,\text{TeV}$ [13].

Writing the operators contained in (1) into $SU(2)_L$-components one can read off couplings to dineutrinos (C_A^M) and to charged dileptons (K_A^M), where $M = U$ ($M = D$) refers to the up-quark sector (down-quark sector) and $A = L(R)$ denotes left- (right-) handed quark currents

$$\begin{aligned} C_L^U = K_L^D &= \frac{2\pi}{\alpha_e}\left(C_{\ell q}^{(1)} + C_{\ell q}^{(3)}\right), C_R^U = K_R^U = \frac{2\pi}{\alpha_e}C_{\ell u}\,, \\ C_L^D = K_L^U &= \frac{2\pi}{\alpha_e}\left(C_{\ell q}^{(1)} - C_{\ell q}^{(3)}\right), C_R^D = K_R^D = \frac{2\pi}{\alpha_e}C_{\ell d}\,, \end{aligned}$$

where α_e denotes the fine-structure constant. The loop factor in the implicit definitions of C_A^M, K_A^M is included to

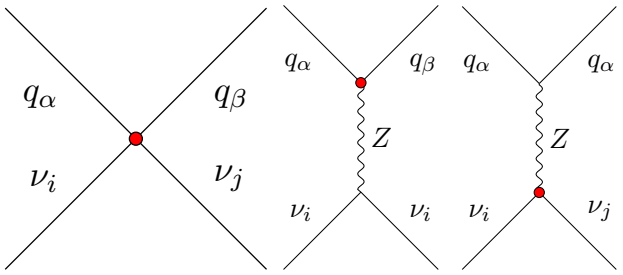

Fig. 1 Contributions of four-fermion operators (1), left-most diagram, and subleading ones involving Z-exchange, see text, to quark q processes into neutrinos, contained in the left-handed lepton doublet, with flavor indices α, β, i, j. Operators are denoted by a blob

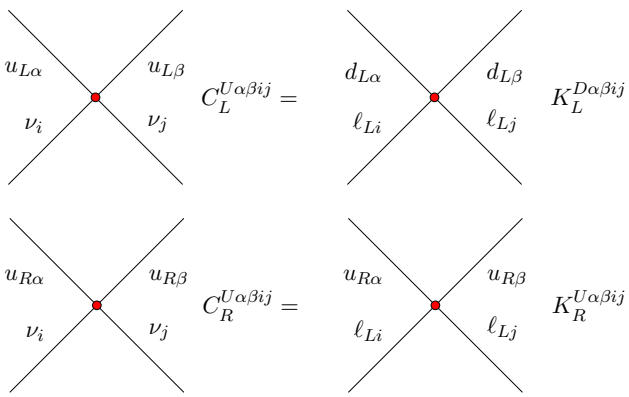

Fig. 2 NP contributions to up and down quark transitions with dineutrinos $C_{L,R}^U$ and dileptons K_L^D and K_R^U, from the operators (1) in the fermions' flavor basis, with flavor indices α, β, i, j. The $SU(2)_L$-based relation between neutrino and charged lepton operators is exploited in (2) in the mass eigenstate basis

facilitate matching onto the weak effective theory, $\mathcal{L} = 4\,G_F/\sqrt{2}\,(\alpha_e/4\pi)\sum C_i\,O_i$. One observes that $C_R^M = K_R^M$. While C_L^M is not fixed in general by K_L^M due to the different relative signs between $C_{\ell q}^{(1)}$ and $C_{\ell q}^{(3)}$, C_L^U is related to K_L^D and C_L^D to K_L^U. This link is visualized in Fig. 2.

Going to mass eigenstates $Q_\alpha = (u_{L\alpha}, V_{\alpha\beta}d_{L\beta})$, $L_i = (\nu_{Li}, W_{ki}^*\ell_{Lk})$ with the Cabibbo-Kobayashi-Maskawa (CKM) and Pontecorvo-Maki-Nakagawa-Sakata (PMNS) matrices V and W, respectively, and summing lepton flavors i, j incoherently, we obtain the trace identity

$$\begin{aligned}\sum_{\nu=i,j}\left(|\mathcal{C}_L^{Mij}|^2+|\mathcal{C}_R^{Mij}|^2\right) &= \mathrm{Tr}\left[\mathcal{C}_L^M\,\mathcal{C}_L^{M\dagger}+\mathcal{C}_R^M\,\mathcal{C}_R^{M\dagger}\right]\\ &= \mathrm{Tr}\left[\mathcal{K}_L^N\mathcal{K}_L^{N\dagger}+\mathcal{K}_R^M\mathcal{K}_R^{M\dagger}\right]+\mathcal{O}(\lambda)\\ &= \sum_{\ell=i,j}\left(|\mathcal{K}_L^{Nij}|^2+|\mathcal{K}_R^{Mij}|^2\right)+\mathcal{O}(\lambda)\,, \end{aligned} \tag{2}$$

between charged lepton couplings $\mathcal{K}_{L,R}$ and neutrino ones $\mathcal{C}_{L,R}$, with Wolfenstein parameter $\lambda \simeq 0.2$. In (2), $M = U$ and $N = D$ if the link is exploited for neutrino couplings in the up-quark sector, as illustrated in Fig. 2, while $M = D$ and $N = U$ for dineutrinos coupling to down-type quarks. Wilson coefficients in calligraphic style denote those for mass eigenstates. Relation (2) follows from $\mathcal{C}_L^M = W^\dagger\,\mathcal{K}_L^N\,W + \mathcal{O}(\lambda)$, $\mathcal{C}_R^M = W^\dagger\,\mathcal{K}_R^M\,W$ using unitarity. The traces in (2) are over the leptonic flavor indices of the Wilson coefficients. In the limit $V = 1$, or for $\mathcal{C}_L = \mathcal{K}_L = 0$, (2) becomes an identity. The lepton flavor indices i, j are spelled out explicitly in (2), while those for the quarks are kept fixed, *e.g.,* $\alpha = u$, $\beta = c$ for $c \to u\,\nu\bar{\nu}$, and are not given to avoid clutter. The correction from CKM-rotation for processes involving third and second, (third and first) generations arise at $\mathcal{O}(\lambda^2)$ (at $\mathcal{O}(\lambda^3)$) if first and second generation mixing can be neglected.

The relation (2) allows to predict dineutrino rates for different leptonic flavor structures $\mathcal{K}_{L,R}^{Mij}$ that can be probed with lepton-specific measurements. We identify the following possibilities:

i) $\mathcal{K}_{L,R}^{Mij} \propto \delta_{ij}$, that is, *lepton-universality* (LU).
ii) $\mathcal{K}_{L,R}^{Mij}$ are diagonal, that is, *charged lepton flavor conservation* (cLFC).
iii) $\mathcal{K}_{L,R}^{Mij}$ general, including *charged lepton flavor violation* (cLFV).

Note, *ii)* relies on the charged lepton mass basis. In the following we discuss implications for different quark sectors. We therefore reinstall quark flavor indices and employ the notation $\mathcal{K}_{L,R}^{tcij} = \mathcal{K}_{L,R}^{U_{23}ij}$, $\mathcal{K}_{L,R}^{bsij} = \mathcal{K}_{L,R}^{D_{23}ij}$, $\mathcal{C}_{L,R}^{bsij} = \mathcal{C}_{L,R}^{D_{23}ij}$, and so on.

Limits on the couplings of semileptonic four-fermion operators $\mathcal{K}_{L,R}^{Mij}$ arise from rare decays, and Drell–Yan production. They are compiled in Tables 1 and 2 (strange and charm), and Tables 4, 5, 6 and 7 (bottom and top), with details given in the next sections.

3 First and second generation quarks

We exploit the $SU(2)_L$-link between strange and charm. Constraints on rare K decays are much stronger than those on charm hadrons such that the former provides input –obtained

Table 1 Upper limits on charged dilepton couplings $\mathcal{K}_A^{sd\ell\ell'}$ from high–p_T [14,15] (top row), charged dilepton K-decays (mid) and derived ones from K decays to dineutrinos (bottom). Numbers correspond to a limit on the modulus. LFV-bounds are quoted as flavor-summed, $\sqrt{|\mathcal{K}^{\ell^+\ell'^-}|^2+|\mathcal{K}^{\ell^-\ell'^+}|^2}$. [a]Obtained assuming no large cancellations between $\mathcal{K}_R^{sd}$ and $\mathcal{K}_L^{cu}$

$sd\ell\ell'$	ee	$\mu\mu$	$\tau\tau$	$e\mu$	$e\tau$	$\mu\tau$
$\lvert\mathcal{K}_{L,R}^{sd\ell\ell'}\rvert_{\mathrm{DY}}$	3.5	1.9	6.7	2.0	6.1	6.6
$\lvert\mathcal{K}_{L,R}^{sd\ell\ell'}\rvert$	$5\cdot10^{-2}$	$1.6\cdot10^{-2}$	–	$6.6\cdot10^{-4}$	–	–
$\lvert\mathcal{K}_R^{sd\ell\ell'}\rvert_{\nu\bar{\nu}}^a$	$[-1.9, 0.7]\cdot10^{-2}$	$[-1.9, 0.7]\cdot10^{-2}$	$[-1.9, 0.7]\cdot10^{-2}$	$1.1\cdot10^{-2}$	$1.1\cdot10^{-2}$	$1.1\cdot10^{-2}$

Table 2 Upper limits on charged dilepton couplings $\mathcal{K}_A^{cu\ell\ell'}$ from high–p_T [14,15] (top row), charged dilepton D-decays [19,20] (mid) and derived ones from kaon decays to dineutrinos (bottom). Numbers correspond to a limit on the modulus. LFV-bounds are quoted as flavor-summed, $\sqrt{|\mathcal{K}^{\ell^+\ell'^-}|^2+|\mathcal{K}^{\ell^-\ell'^+}|^2}$. [†] No limit on $D^0 \to e^\pm\tau^\mp$ available. [a]Obtained assuming no large cancellations between $\mathcal{K}_R^{sd}$ and $\mathcal{K}_L^{cu}$

$cu\ell\ell'$	ee	$\mu\mu$	$\tau\tau$	$e\mu$	$e\tau$	$\mu\tau$
$\lvert\mathcal{K}_{L,R}^{cu\ell\ell'}\rvert_{\mathrm{DY}}$	2.9	1.6	5.6	1.6	4.7	5.1
$\lvert\mathcal{K}_{L,R}^{cu\ell\ell'}\rvert$	4.0	0.9	–	2.2	n.a.[†]	–
$\lvert\mathcal{K}_L^{cu\ell\ell'}\rvert_{\nu\bar{\nu}}^a$	$[-1.9, 0.7]\cdot10^{-2}$	$[-1.9, 0.7]\cdot10^{-2}$	$[-1.9, 0.7]\cdot10^{-2}$	$1.1\cdot10^{-2}$	$1.1\cdot10^{-2}$	$1.1\cdot10^{-2}$

in Sec. 3.1 – for universality and cLFC tests with $c \to u\nu\bar{\nu}$ processes, discussed in Sec. 3.2.

3.1 Kaon constraints

$SU(2)_L$ connects $s \to d\,\nu\bar{\nu}$ branching ratios with charged dilepton couplings $\mathcal{K}_L^{cu\ell\ell'}$ and $\mathcal{K}_R^{sd\ell\ell'}$. Using Ref. [16] and Eq. (2), we obtain

$$\mathcal{B}(K^+ \to \pi^+ \nu\bar{\nu}) = A_+^{K^+\pi^+} \cdot x_{sd}^+ \,, \tag{3}$$

where $A_+^{K^+\pi^+} = (68.0 \pm 1.9) \cdot 10^{-8}$ [17], and

$$x_{sd}^+ = \sum_{i,j} \left| \mathcal{C}_{\rm SM}^{sd}\delta_{ij} + \mathcal{K}_L^{cuij} + \mathcal{K}_R^{sdij} \right|^2 , \tag{4}$$

Table 3 Coefficients $A_\pm^{h_c F}$, as defined in (15), and model-independent upper limits on $\mathcal{B}_{\rm LU}^{\rm max}$, $\mathcal{B}_{\rm cLFC}^{\rm max}$, $\mathcal{B}^{\rm max}$ from (11), (12) and (13), respectively, corresponding to the lepton flavor symmetry benchmarks *i)-iii)*. The first two columns are taken from Ref. [22]

$h_c \to F$	$A_+^{h_c F}$ $[10^{-8}]$	$A_-^{h_c F}$ $[10^{-8}]$	$\mathcal{B}_{\rm LU}^{\rm max}$ $[10^{-7}]$	$\mathcal{B}_{\rm cLFC}^{\rm max}$ $[10^{-6}]$	$\mathcal{B}^{\rm max}$ $[10^{-6}]$
$D^0 \to \pi^0$	0.9	–	0.5	2.8	12
$D^+ \to \pi^+$	3.6	–	1.9	11	47
$D_s^+ \to K^+$	0.7	–	0.3	2.1	8.8
$D^0 \to \pi^0\pi^0$	$\mathcal{O}(10^{-3})$	0.21	0.1	0.7	2.8
$D^0 \to \pi^+\pi^-$	$\mathcal{O}(10^{-3})$	0.41	0.2	1.3	5.4
$D^0 \to K^+K^-$	$\mathcal{O}(10^{-6})$	0.004	0.002	0.01	0.06
$\Lambda_c^+ \to p^+$	1.0	1.7	1.4	8.4	35
$\Xi_c^+ \to \Sigma^+$	1.8	3.5	2.7	17	70
$D^0 \to X$	2.2	2.2	1.1	6.9	29
$D^+ \to X$	5.6	5.6	2.9	17	74
$D_s^+ \to X$	2.7	2.7	1.4	8.3	35

Table 4 Upper limits on charged dilepton couplings $\mathcal{K}_A^{bs\ell\ell'}$ from high–p_T [14,15] (top row), charged dilepton B-decays (middle rows) and derived ones from three-body rare B-decays to dineutrinos (bottom). Numbers without ranges correspond to a limit on the modulus. the $\mu\mu$ ranges are obtained from a global fit, with the departures from zero in $\mathcal{K}_L^{bs\mu\mu}$ corresponding to the flavor anomaly. LFV-bounds are quoted as flavor-summed, $\sqrt{|\mathcal{K}^{\ell^+\ell'^-}|^2 + |\mathcal{K}^{\ell^-\ell'^+}|^2}$, whereas the other bounds are for a single coupling

$bs\ell\ell'$	ee	$\mu\mu$	$\tau\tau$	$e\mu$	$e\tau$	$\mu\tau$
$\lvert\mathcal{K}_{L,R}^{bs\ell\ell'}\rvert_{\rm DY}$	13	7.1	25	8.0	27	30
$\mathcal{K}_R^{bs\ell\ell'}$	0.04	$[-0.03; -0.01]$	32	0.1	2.8	3.4
$\mathcal{K}_L^{bs\ell\ell'}$	0.04	$[-0.06; -0.04]$	32	0.1	2.8	3.4
$\mathcal{K}_R^{bs\ell\ell'}\rvert_{\nu\bar{\nu}}$	1.4	1.4	1.4	1.8	1.8	1.8

Table 5 Upper limits on charged dilepton couplings $\mathcal{K}_A^{bd\ell\ell'}$ from high–p_T [14,15] (top row), charged dilepton B-decays (middle rows) and derived ones from three-body rare B-decays to dineutrinos (bottom). Numbers without ranges correspond to a limit on the modulus. The $\mu\mu$ ranges are obtained from a global fit. LFV-bounds are quoted as flavor-summed, $\sqrt{|\mathcal{K}^{\ell^+\ell'^-}|^2 + |\mathcal{K}^{\ell^-\ell'^+}|^2}$, whereas the other bounds are for a single coupling

$bd\ell\ell'$	ee	$\mu\mu$	$\tau\tau$	$e\mu$	$e\tau$	$\mu\tau$
$\lvert\mathcal{K}_{L,R}^{bd\ell\ell'}\rvert_{\rm DY}$	5.0	2.7	9.6	3.1	9.6	11
$\mathcal{K}_R^{bd\ell\ell'}$	0.09	$[-0.03, 0.03]$	21	0.2	3.4	2.4
$\mathcal{K}_L^{bd\ell\ell'}$	0.09	$[-0.07, 0.02]$	21	0.2	3.4	2.4
$\mathcal{K}_R^{bd\ell\ell'}\rvert_{\nu\bar{\nu}}$	1.8	1.8	1.8	2.5	2.5	2.5

with [17]

$$\mathcal{C}_{\rm SM}^{sd} = 0.0059 - 0.0017\,{\rm i}\,. \tag{5}$$

Translating the current measurement $\mathcal{B}(K^+ \to \pi^+\nu\bar{\nu})_{\rm exp} = \left(8^{+6}_{-4}\right) \cdot 10^{-11}$ [18] into the 90% CL upper limit $\mathcal{B}(K^+ \to \pi^+\nu\bar{\nu})_{\rm exp} \lesssim 1.7 \cdot 10^{-10}$ yields

$$x_{sd}^+ \lesssim 2.5 \cdot 10^{-4}\,. \tag{6}$$

Employing Eqs. (5) and (6), we can extract limits on the couplings $\mathcal{K}_L^{cu}$ and $\mathcal{K}_R^{sd}$. Since there is only sensitivity to the sum of these couplings, we assume that there are no large cancellations and derive bounds only on one coupling at a time. In the LU limit, we obtain the following limit

$$-0.015 \lesssim \mathcal{K}_L^{cu\ell\ell}, \mathcal{K}_R^{sd\ell\ell} \lesssim 0.003\,, \quad \ell = e, \mu, \tau\,. \tag{7}$$

Assuming only a single non-vanishing, flavor-conserving contribution, assumed here for concreteness to be for ditaus, the strongest limits corresponding to cLFC read

$$-0.019 \lesssim \mathcal{K}_L^{cu\tau\tau}, \mathcal{K}_R^{sd\tau\tau} \lesssim 0.007\,. \tag{8}$$

Finally, we also consider the case where only one non-diagonal (LFV) coupling is switched on, *e.g.* $\mathcal{K}_{L,R}^{\tau e} = \mathcal{K}_{L,R}^{e\tau}$, which yields

$$|\mathcal{K}_L^{cu\ell\ell'}|, |\mathcal{K}_R^{sd\ell\ell'}| \lesssim 0.008\,, \quad \text{for} \quad \ell \neq \ell'\,. \tag{9}$$

Comparing these bounds with the corresponding limits from high-p_T in Tables 1 and 2, we observe that dineutrino data provides stronger constraints, by several orders of magnitude on left-handed $c \to u$ and right-handed $s \to d$ dilepton couplings. Limits from charged dilepton data (mid rows in Tables 1, 2) are worked out as well using Refs. [16,19,20].

The strongest limits on the real part of $s\,d\,e^+\,e^-$ and $s\,d\,\mu^+\,\mu^-$ couplings are set by $K_L^0 \to e^+e^-$ and $K_L^0 \to$

$\mu^+\mu^-$ decays, while the strongest limit on the imaginary part is provided by $K_L^0 \to \pi^0 e^+ e^-$ and $K_L^0 \to \pi^0 \mu^+ \mu^-$ decays. The numbers in Table 1 are quoted as the absolute values. We also provide limits on $s\,d\,\mu\,e$ couplings which result from $K_L^0 \to e^\pm \mu^\mp$. In $s \to d$ transitions, dineutrino modes provide the strongest constraints on modes with taus, $\tau^+\tau^-$, $\tau\mu$, and τe which again are kinematically not accessible from kaon decays to charged dileptons.

3.2 Predictions for charm

Here we discuss the ramifications of (2) for $c \to u\,\nu\bar{\nu}$ processes, which constitute clean null tests of the SM. We show that branching ratios of rare charm hadron decays to dineutrinos cannot exceed upper limits for a given lepton flavor benchmark *i)-iii)*. The situation for $c \to u\,\nu\bar{\nu}$ dineutrino transitions is quite unique as the SM amplitude is entirely negligible due to an efficient GIM-cancellation [5] and the current lack of experimental constraints.[1] Further details can be found in Ref. [22].

Since the neutrino flavors are not tagged, as common to generic particle physics experiments, a dineutrino branching ratio is an incoherent sum of flavor-specific ones

$$\mathcal{B}\,(c \to u\,\nu\bar{\nu}) = \sum_{i,j} \mathcal{B}\left(c \to u\,\nu_i\bar{\nu}_j\right) \propto x_{cu}\,,$$
$$x_{cu} = \sum_{i,j} |\mathcal{C}_L^{Uij}|^2 + |\mathcal{C}_R^{Uij}|^2\,. \tag{10}$$

Using (2) with $M = U$ and $N = D$ and the constraints on $|\Delta s| = |\Delta d| = 1$ and $|\Delta c| = |\Delta u| = 1$ couplings given in Tables 1 and 2 we obtain upper limits in the lepton flavor benchmarks *i)-iii)*:

$$x_{cu} = 3\,x_{cu}^{\mu\mu} \lesssim 2.6\,, \quad \text{(LU)} \tag{11}$$
$$x_{cu} = x_{cu}^{ee} + x_{cu}^{\mu\mu} + x_{cu}^{\tau\tau} \lesssim 156\,, \quad \text{(cLFC)} \tag{12}$$
$$x_{cu} = x^{ee} + x_{cu}^{\mu\mu} + x_{cu}^{\tau\tau} + 2(x_{cu}^{e\mu} + x_{cu}^{e\tau} + x_{cu}^{\mu\tau}) \lesssim 655\,. \tag{13}$$

Here, the flavor-specific contributions $x_{cu}^{\ell\ell'} = |\mathcal{K}_L^{sd\ell\ell'}|^2 + |\mathcal{K}_R^{cu\ell\ell'}|^2 + \mathcal{O}(\lambda)$, where $x_{cu} = \sum_{\ell,\ell'} x_{cu}^{\ell\ell'}$, to each upper limit have been spelled out. Since dimuon bounds are the most stringent ones they govern the LU-limit (11). Note also that subleading CKM-corrections are included in (11)–(13) [22].

In contrast to Ref. [22] we use low energy constraints on the couplings $\mathcal{K}_A^{qq'\ell\ell'}$ in addition to the high-p_T ones, *i.e.* we use the strongest available limits on $\mathcal{K}_{L,R}^{sd\ell\ell'}$ and $\mathcal{K}_{L,R}^{cu\ell\ell'}$ from Tables 1 and 2. The inclusion of rare kaon data implies improved bounds in Eqs. (11), (12), (13) and Table 3 with respect to the results in Ref. [22].

Various exclusive dineutrino branching ratios depend on combinations of left and right quark chiralities,

$$x_{cu}^{\pm} = \sum_{i,j} |\mathcal{C}_L^{cuij} \pm \mathcal{C}_R^{cuij}|^2 \tag{14}$$

with $x_{cu}^+ + x_{cu}^- = 2x_{cu}$, hence both $x_{cu}^\pm$ are bounded by x_{cu}. Specifically, x_{cu}^+ arises in the $D \to P\,\nu\bar{\nu}$ branching ratio, whereas $D \to P\,P'\,\nu\bar{\nu}$, $P, P' = \pi, K$, branching ratios are dominated by x_{cu}^-. Inclusive decays and, approximately, the baryonic ones are dominated by x_{cu}. All branching ratios of a charmed hadron h_c into a final hadron F and dineutrinos can be written as

$$\mathcal{B}(h_c \to F\,\nu\bar{\nu}) = A_+^{h_c F}\,x_{cu}^+ + A_-^{h_c F}\,x_{cu}^-\,, \tag{15}$$

with $A_\pm^{h_c F}$ coefficients [22] compiled in Table 3. Experimental extraction of x_{cu} or $x_{cu}^\pm \le 2\,x_{cu}$ above the upper limit in (11) would indicate a breakdown of LU, whereas values above (12) would imply cLFV. We also obtain achievable, total upper limits in (13). Corresponding upper limits on branching ratios of rare charm dineutrino modes are given in Table 3.

We recall that $c \to u$ dineutrino FCNCs require the presence of NP to be observable. Due to their strong ties with the charged dilepton modes, dineutrino modes are not only clean probes of BSM physics, their rate is informative on lepton flavor.

4 Third generation quarks

We summarize predictions (Sect. 4.1) and tests (Sect. 4.2) for beauty decays and work out predictions and opportunities for the top sector in Sects. 4.3 and 4.4.

4.1 Predictions for beauty

In this section we study $b \to q\,\nu\bar{\nu}$ transitions and their interplay with $b \to q\,\ell^+\ell^-$ transitions routed by (2). First, we use SM effective theory to improve the limits on charged ditau couplings from dineutrino data. Finally, we exploit Eq. (2) using the complementarity between $B \to V$ and $B \to P$ dineutrino branching ratios, which offers novel tests of lepton universality. Further details can be found in Ref. [13].

Using the current experimental 90 % CL upper limits [18]

$$\mathcal{B}(B^0 \to K^{*0}\nu\bar{\nu})_{\text{exp}} < 18 \cdot 10^{-6}\,,$$
$$\mathcal{B}(B^+ \to K^+\nu\bar{\nu})_{\text{exp}} < 16 \cdot 10^{-6}\,, \tag{16}$$

[1] The $D^0 \to \nu\bar{\nu}$ branching ratio induced by (axial-)vector operators is helicity suppressed by two powers of neutrino mass, and negligible. The Belle result $\mathcal{B}(D^0 \to \nu\bar{\nu}) < 9.4 \cdot 10^{-5}$ at 90% CL [21] can therefore be safely avoided.

$$\mathcal{B}(B^+ \to \rho^+ \nu\bar{\nu})_{\rm exp} < 30 \cdot 10^{-6}\,,$$
$$\mathcal{B}(B^+ \to \pi^+ \nu\bar{\nu})_{\rm exp} < 14 \cdot 10^{-6}\,, \tag{17}$$

one can extract the following bounds on $x_{bq}^{\pm}$ [13]

$$x_{bs}^{+} \lesssim 2.9, \qquad x_{bs}^{-} + 0.2\, x_{bs}^{+} \lesssim 2.0\,, \tag{18}$$
$$x_{bd}^{+} \lesssim 4.2, \qquad x_{bd}^{-} + 0.1\, x_{bd}^{+} \lesssim 2.4\,, \tag{19}$$

where

$$x_{bs}^{\pm} = \sum_{i,j} \left| \mathcal{C}_{\rm SM}^{bs}\, \delta_{ij} + \mathcal{K}_L^{tcij} \pm \mathcal{K}_R^{bsij} \right|^2\,,$$
$$x_{bd}^{\pm} = \sum_{i,j} \left| \mathcal{C}_{\rm SM}^{bd}\, \delta_{ij} + \mathcal{K}_L^{tuij} \pm \mathcal{K}_R^{bdij} \right|^2\,. \tag{20}$$

These are the analogues of (14) for beauty and include the finite SM contribution $\mathcal{C}_{\rm SM}^{bs} = 0.50 - 0.01\,{\rm i}$ and $\mathcal{C}_{\rm SM}^{bd} = -0.10 - 0.04\,{\rm i}$.

The limits (18) and (19) allow one to set bounds on $\mathcal{K}_L^{tc(u)ij}$, $\mathcal{K}_R^{bs(d)ij}$ via Eq. (20), depending on the lepton flavor assumptions. We observe that limits from charged lepton data are stronger or similar than the dineutrino bounds with the exception of $\tau\tau$ and $e\tau$ for $b \to d$, [13]

$$|\mathcal{K}_R^{bd\tau\tau}| \lesssim 1.8\,, \quad |\mathcal{K}_R^{bde\tau}| \lesssim 2.5\,, \tag{21}$$

and $e\tau$, $\mu\tau$, $\tau\tau$ for $b \to s$

$$|\mathcal{K}_R^{bs\tau\ell}| \lesssim 1.4\,, \qquad |\mathcal{K}_R^{bs\tau\tau}| \lesssim 1.8\,. \tag{22}$$

Notice that dineutrino limits are stronger than those from Drell–Yan data, cf. Tables 4 and 5. The constraints on the top FCNCs following from the same analysis are given in Tables 6 and 7.

4.2 Testing universality with $b \to q\,\nu\bar{\nu}$

The branching ratios for $B \to V\,\nu\bar{\nu}$ and $B \to P\,\nu\bar{\nu}$ decays in the lepton universality limit are given by

$$\mathcal{B}(B \to V\,\nu\bar{\nu})_{\rm LU} = A_+^{BV}\, x_{bq,{\rm LU}}^{+} + A_-^{BV}\, x_{bq,{\rm LU}}^{-}\,, \tag{23}$$
$$\mathcal{B}(B \to P\,\nu\bar{\nu})_{\rm LU} = A_+^{BP}\, x_{bq,{\rm LU}}^{+}\,, \tag{24}$$

respectively, with $x_{bq,{\rm LU}}^{\pm} = 3\left|\mathcal{C}_{\rm SM}^{bq\ell\ell} + \mathcal{K}_L^{tq'\ell\ell} \pm \mathcal{K}_R^{bq\ell\ell}\right|^2$, with $q' = u$, (c) for $q = d$, (s), respectively, and ℓ fixed to the flavor with strongest constraints. Since present rare top data are not able to put useful constraints on the coupling $\mathcal{K}_L^{tq'\ell\ell}$, we instead solve $\mathcal{B}(B \to P\,\nu\bar{\nu})_{\rm LU}$ in Eq. (24) for $\mathcal{K}_L^{tq'\ell\ell}$ and plug the two solutions into Eq. (23). This yields a correlation between the branching ratios,

$$\mathcal{B}(B \to V\,\nu\bar{\nu})_{\rm LU} = \frac{A_+^{BV}}{A_+^{BP}}\,\mathcal{B}(B \to P\,\nu\bar{\nu})_{\rm LU} + 3\,A_-^{BV}\left|\sqrt{\frac{\mathcal{B}(B \to P\,\nu\bar{\nu})_{\rm LU}}{3\,A_+^{BP}}} \mp 2\,\mathcal{K}_R^{bq\ell\ell}\right|^2\,. \tag{25}$$

The most stringent limits on $\mathcal{K}_R^{bq\ell\ell}$ are given for muons. By performing a six-dimensional global fit of the semi-leptonic Wilson coefficients $\mathcal{C}^{(\prime)}_{(7,9,10),\mu}$ to current experimental information on $b \to s\,\mu^+\mu^-$ data (excluding $R_{K^{(*)}}$ which can be polluted by NP effects in electron couplings), we obtain the following 1σ fit values [13,23]

$$\mathcal{K}_R^{bs\mu\mu} = V_{tb}V_{ts}^*\,(0.46 \pm 0.26)\,, \tag{26}$$
$$\mathcal{K}_R^{bd\mu\mu} = V_{tb}V_{td}^*\,(0 \pm 4)\,. \tag{27}$$

Figure 3 displays the correlation between $\mathcal{B}(B^0 \to K^{*0}\nu\bar{\nu})$ and $\mathcal{B}(B^0 \to K^0\nu\bar{\nu})$ using Eq. (25), with $\mathcal{K}_R^{bs\mu\mu}$ from Eq. (26). Scanning $\mathcal{K}_R^{bs\mu\mu}$, and the form factors [13] $A_+^{B^0K^{*0}} = (200 \pm 29)\cdot 10^{-8}$, $A_-^{B^0K^{*0}} = (888 \pm 108)\cdot 10^{-8}$, $A_+^{B^0K^0} = (516 \pm 68)\cdot 10^{-8}$, within their $1\,\sigma$ $(2\,\sigma)$ regions, one obtains

$$\frac{\mathcal{B}(B^0 \to K^{*0}\nu\bar{\nu})_{\rm LU}}{\mathcal{B}(B^0 \to K^0\nu\bar{\nu})_{\rm LU}} = 1.7\ldots2.6 \quad (1.3\ldots2.9)\,, \tag{28}$$

displayed by the red region. Measurements outside this region would signal a breakdown of LU. Note, however, that a measurement inside this region does not necessarily imply LU. The SM predictions

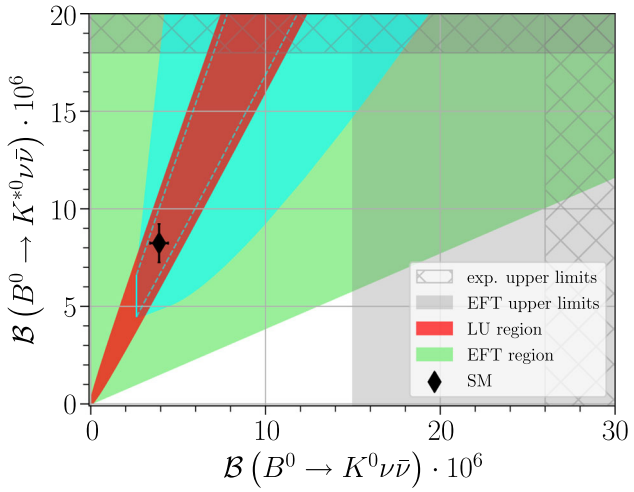

Fig. 3 $\mathcal{B}(B^0 \to K^{*0}\,\nu\bar{\nu})$ versus $\mathcal{B}(B^0 \to K^0\,\nu\bar{\nu})$. SM predictions with uncertainties (black) from (29). The red region represents the LU region (25) at $1\,\sigma$, and it is mainly dominated from form factor uncertainties. The green region represents the validity of the EFT framework, given by Eq. (18). Cyan region represents cLFC region for a single species, in particular $\ell = \tau$, assuming a bound on $\mathcal{B}(B_s^0 \to \tau^+\tau^-) \lesssim 10^{-6}$. Dashed cyan lines represent the cLFC region for $\ell = \mu$, see main text

$$\begin{aligned}\mathcal{B}(B^0 \to K^{*0}\nu\bar{\nu})_{\rm SM} &= (8.2 \pm 1.0)\cdot 10^{-6}\,,\\ \mathcal{B}(B^0 \to K^{0}\nu\bar{\nu})_{\rm SM} &= (3.9 \pm 0.5)\cdot 10^{-6}\,,\end{aligned} \tag{29}$$

are depicted with their uncertainties (black). The green region represents the validity of our effective field theory (EFT) framework, given by Eq. (18). The hatched bands correspond to current experimental 90 % CL upper limits (16). The gray bands represent the derived EFT limits, $\mathcal{B}(B^0 \to K^0\nu\bar{\nu})_{\rm derived} < 1.5\cdot 10^{-5}$ [13]. A measurement between gray and hatched area would imply BSM physics not covered by the EFT framework. Belle II is expected to observe these modes with 50 ab^{-1} and 10% accuracy. Similar conclusions are found in $b \to d\,\nu\bar{\nu}$ decay, a detailed analysis can be found in Ref. [13].

The possibility of testing cLFC mainly depends on $\mathcal{K}_R^{bs\tau\tau}$ constraints. Currently, the bounds provided by dineutrino modes are a factor 23 stronger than direct limits from $\mathcal{B}(B_s^0 \to \tau^+\tau^-)$, see Table 4. Working out the projections from Belle II with 5 ab^{-1}, $\mathcal{B}(B_s^0 \to \tau^+\tau^-)_{\rm proj} \le 8.1\cdot 10^{-5}$ [24], we observe that dineutrino limits would still be a factor 3 stronger. In contrast if the direct experimental limit would be two orders of magnitude stronger $\mathcal{B}(B_s^0 \to \tau^+\tau^-) \lesssim 10^{-6}$, testing cLFC would be possible. Figure 3 displays precisely the cLFC limit for single species (ℓ fixed), that is $x_{bs}^{\pm} = 2\left|\mathcal{C}_{\rm SM}^{bs}\right|^2 + \left|\mathcal{C}_{\rm SM}^{bs} + \mathcal{K}_L^{tc\ell\ell} \pm \mathcal{K}_R^{bs\ell\ell}\right|^2$. For $\ell = \tau$ (filled cyan region), we assume $\mathcal{B}(B_s^0 \to \tau^+\tau^-) \lesssim 10^{-6}$, which implies a constraint on $\mathcal{K}_R^{bs\tau\tau}$, while $\mathcal{K}_L^{tc\tau\tau}$ remains unconstrained. The filled cyan region is then obtained by varying $\mathcal{K}_R^{bs\tau\tau}$ and $\mathcal{K}_L^{tc\tau\tau}$. A measurement outside of this region implies a violation of cLFC in the limit of large $\tau\tau$ couplings. We have also studied $\ell = \mu$ indicated by the dashed cyan lines, where the corresponding region lies inside the LU region, because $\mathcal{K}_R^{bs\mu\mu}$ is strongly bounded from $b \to s\mu\mu$ global fits. Note that assuming cLFC for a single species, the region is bounded from below as $x_{bs}^{\pm} \ge 2\,|\mathcal{C}_{\rm SM}^{bs}|^2$ (cyan solid line), implying a lower limit on the branching ratios of 2/3 of the SM one.

4.3 Predictions for top

The $SU(2)_L$–link connects left-handed quark couplings in $b \to s\ell\ell^{(\prime)}$ and $b \to d\ell\ell^{(\prime)}$ observables to left-handed tc– and tu–dineutrino couplings, respectively. Constraints on the former, $\mathcal{K}_L^{bsij}$ and $\mathcal{K}_L^{bdij}$, are available for all lepton flavors i, j, see Tables 4 and 5. Constraints on right-handed contributions $\mathcal{K}_R^{tqij}$ are much weaker. The most stringent ones available are on cLFV couplings. CMS [25] provides upper limits on $e\mu$ final states, corresponding to rare top branching ratios

$$\begin{aligned}\mathcal{B}(t \to u\,e^+\mu^- + u\,e^-\mu^+)_{\rm exp} &< 0.135\cdot 10^{-6}\,,\\ \mathcal{B}(t \to c\,e^+\mu^- + c\,e^-\mu^+)_{\rm exp} &< 1.31\cdot 10^{-6}\,.\end{aligned} \tag{30}$$

ATLAS [26] also provides bounds on cLFV modes involving taus (at 95 % CL)

$$\mathcal{B}(t \to q\,\tau\,(e,\mu))_{\rm exp} < 1.86\cdot 10^{-5}\,,\quad q = u, c\,, \tag{31}$$

which we scaled to arrive at the constraints on the Wilson coefficients in Tables 6 and 7. We also employ limits on an admixture of $ttee$ and $tt\mu\mu$ couplings [27] as upper limits on the FCNC ones $tq\ell\ell$, $|\mathcal{K}_{L,R}^{tq\ell\ell}| \lesssim |\mathcal{K}_{L,R}^{tt\ell\ell}| \lesssim 200$ for $\ell = e, \mu$. This is consistent with the rare mode being considered as a signal in the search. Projected limits for 140 fb^{-1} of LHC data in single top production in association with dimuons [28] would yield $|\mathcal{K}_{L,R}^{tc\mu\mu}| \lesssim 40$ and $|\mathcal{K}_{L,R}^{tu\mu\mu}| \lesssim 4.8$. These are stronger than the $tt\mu\mu$ constraints, and those from LFV $t \to u$ decays (30), (31), but slightly weaker than the ones from LFV $t \to c$ decays. The constraints on the left-handed coefficients from rare B-decays to dineutrinos, denoted in Tables 6 and 7 by $|\mathcal{K}_L^{tq\ell\ell'}|_{\nu\bar{\nu}}$, are the strongest. Note that all chiralities contribute decoherently in the high energy limit where masses are neglected. We are not aware of any data with ditaus.

Table 6 Upper limits on charged dilepton couplings $\mathcal{K}_A^{tc\ell\ell'}$ from collider studies [25–27] of top plus charged dilepton processes (top row), see text, and on charged dilepton couplings $\mathcal{K}_L^{tc\ell\ell'}$ derived from three-body rare B-decays to dineutrinos (bottom row) except when a range is given. Numbers correspond to a limit on the modulus. LFV-bounds are quoted as flavor-summed, $\sqrt{|\mathcal{K}^{\ell^+\ell'^-}|^2 + |\mathcal{K}^{\ell^-\ell'^+}|^2}$

$tc\ell\ell'$	ee	$\mu\mu$	$\tau\tau$	$e\mu$	$e\tau$	$\mu\tau$
$\lvert\mathcal{K}_{L,R}^{tc\ell\ell'}\rvert$	~ 200	~ 200	n.a.	36	136	136
$\lvert\mathcal{K}_L^{tc\ell\ell'}\rvert_{\nu\bar{\nu}}$	$[-1.9, 0.9]$	$[-1.9, 0.9]$	$[-1.9, 0.9]$	1.8	1.8	1.8

Table 7 Upper limits on charged dilepton couplings $\mathcal{K}_A^{tu\ell\ell'}$ from collider studies [25–27] of top plus charged dilepton processes (top row), see text, and on charged dilepton couplings $\mathcal{K}_L^{tu\ell\ell'}$ derived from three-body rare B-decays to dineutrinos (bottom row). Numbers correspond to a limit on the modulus except when a range is given. LFV-bounds are quoted as flavor-summed, $\sqrt{|\mathcal{K}^{\ell^+\ell'^-}|^2 + |\mathcal{K}^{\ell^-\ell'^+}|^2}$

$tu\ell\ell'$	ee	$\mu\mu$	$\tau\tau$	$e\mu$	$e\tau$	$\mu\tau$
$\lvert\mathcal{K}_{L,R}^{tu\ell\ell'}\rvert$	~ 200	~ 200	n.a.	12	136	136
$\lvert\mathcal{K}_L^{tu\ell\ell'}\rvert_{\nu\bar{\nu}}$	$[-1.6, 1.8]$	$[-1.6, 1.8]$	$[-1.6, 1.8]$	2.4	2.4	2.4

By means of (2), $\mathcal{K}_L^{bqij}$ and $\mathcal{K}_R^{tqij}$ enter dineutrino observables in the top-sector

$$x_{tc} = \sum_{i,j} |\mathcal{K}_L^{bsij}|^2 + |\mathcal{K}_R^{tcij}|^2 + \mathcal{O}(\lambda)\,, \tag{32}$$

$$x_{tu} = \sum_{i,j} |\mathcal{K}_L^{bdij}|^2 + |\mathcal{K}_R^{tuij}|^2 + \mathcal{O}(\lambda)\,, \tag{33}$$

where x_{tc} and x_{tu} are defined as in charm (10). The absence of a limit on $\mathcal{K}_R^{tq\tau\tau}$ allows only to test LU. We obtain

$$x_{tq} \lesssim 1.2 \cdot 10^5 \quad (\text{LU})\,, \quad q = u, c\,. \tag{34}$$

Significantly stronger limits, and further predictions are obtained when assuming contributions from left-handed couplings only. We find for $tc\nu\nu$

$$\begin{aligned} x_{tc}^L &\lesssim 0.011 \quad (\text{LU})\,, \\ x_{tc}^L &\lesssim 630 \quad (\text{cLFC})\,, \\ x_{tc}^L &\lesssim 650 \quad (\text{general})\,, \end{aligned} \tag{35}$$

and for $tu\nu\nu$

$$\begin{aligned} x_{tu}^L &\lesssim 0.015 \quad (\text{LU})\,, \\ x_{tu}^L &\lesssim 90 \quad (\text{cLFC})\,, \\ x_{tu}^L &\lesssim 120 \quad (\text{general})\,. \end{aligned} \tag{36}$$

These are the first bounds of this type constraining tc– and tu–dineutrino couplings.

The bounds (34), (35) and (36) imply upper limits on dineutrino branching ratios of FCNC top decays

$$\mathcal{B}(t \to q\nu\bar{\nu}) = \frac{G_F^2 m_t^5}{\Gamma_t 192\pi^3} \left(\frac{\alpha_e}{4\pi}\right)^2 x_{tq} \simeq x_{tq} \cdot 10^{-9}\,, \tag{37}$$

which provide novel tests of LU and cLFC. $\Gamma_t = 1.35\,\text{GeV}$ denotes the top width [18]. LU (34) predicts hence

$$\mathcal{B}(t \to q\nu\bar{\nu})_{\text{LU}} \lesssim 10^{-4}\,. \tag{38}$$

The bound is driven by the poorly known $\mathcal{K}_R^{tq\ell\ell}$ couplings, and much stronger ones are obtained assuming left-handed couplings only

$$\mathcal{B}(t \to c\nu\bar{\nu})_{\text{LU}}^{\text{L}} \lesssim 1 \cdot 10^{-11}\,, \tag{39}$$

$$\mathcal{B}(t \to u\nu\bar{\nu})_{\text{LU}}^{\text{L}} \lesssim 2 \cdot 10^{-11}\,, \tag{40}$$

$SU(2)_L$ connects also $b \to s\nu\bar{\nu}$ and $b \to d\nu\bar{\nu}$ observables to left-handed tc– and tu–couplings with charged leptons, respectively. Corresponding limits are given in Tables 6 and 7.

4.4 Collider tests with single tops

While the tests of LU and cLFC can be performed at the level of top branching ratios (37), we propose tests with single top production at the LHC, at least for the charged lepton couplings as in [25–27], or a future electron [29] or muon [30, 31] collider. Semileptonic four-fermion operators involving $qt\ell\ell'$ or $qt\nu\bar{\nu}$, $q = u, c$ contribute to single top and single top plus jet signatures, shown in Fig. 4.

To begin let us recall that in the high energy limit all chiralities contribute without interference. In this limit, constraints in top plus dilepton measurements appear in the following combination of Wilson coefficients

$$|\mathcal{K}_L^{tq\ell\ell'}|^2 + |\mathcal{K}_R^{tq\ell\ell'}|^2 + |\mathcal{G}_L^{tq\ell\ell'}|^2 + |\mathcal{G}_R^{tq\ell\ell'}|^2\,. \tag{41}$$

Here the couplings $\mathcal{G}_{L,R}$ correspond to additional terms in the SMEFT Lagrangian [8], with $SU(2)_L$-singlet leptons E as $\frac{C_{qe}}{v^2}\bar{Q}\gamma_\mu Q\bar{E}\gamma^\mu E$ and $\frac{C_{ue}}{v^2}\bar{U}\gamma_\mu U\bar{E}\gamma^\mu E$, where

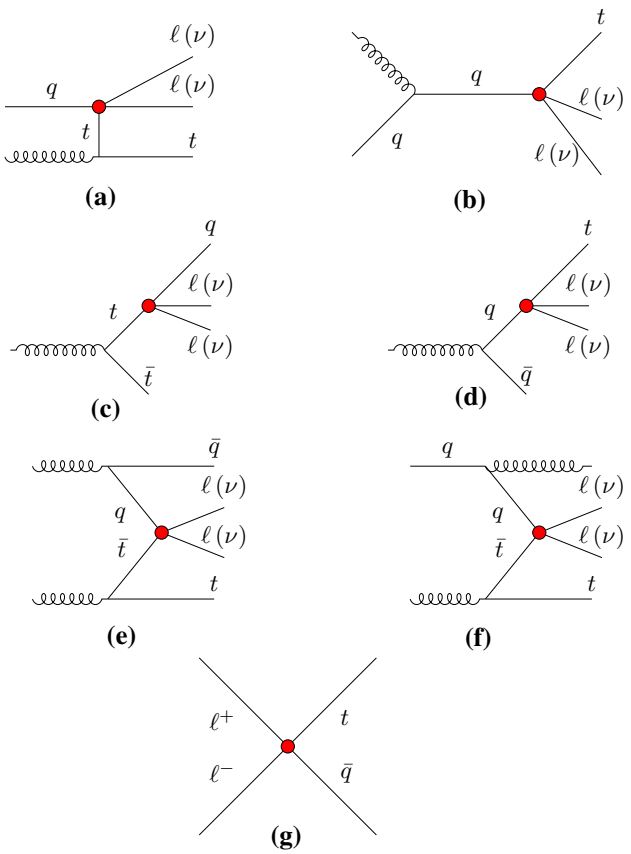

Fig. 4 Diagrams with semileptonic four-fermion operators involving $qt\ell\ell'$ or $qt\nu\bar{\nu}$, $q = u, c$ (red blobs) that contribute to (a)+(b): single top plus dileptons, or single top plus missing energy, wiggly line are gluons, (c)-(f): single top plus jet plus opposite sign dileptons, or single top plus jet plus missing energy. Wiggly lines are gluons, suitable to hadron collider study, or electroweak gauge bosons γ, Z, which can also contribute at a lepton collider (c)+(d). Contribution g) matters only for lepton colliders, with $\ell^+\ell^-$ annihilating into $t\bar{q}$

$\mathcal{G}_L^{U,D} = (2\pi/\alpha_e)C_{qe}$ and $\mathcal{G}_R^U = (2\pi/\alpha_e)C_{ue}$. The couplings to $SU(2)_L$-doublet quarks $\mathcal{G}_L^{tq\ell\ell'}$ are subjected to bounds on right-handed leptons from B-decay via the weak effective theory coefficients $\sim C_9^{\ell\ell'} + C_{10}^{\ell\ell'}$, resulting in $\mathcal{G}_L^{tc\mu\mu} = V_{tb}V_{ts}^*(-0.02 \pm 0.49) \sim 0.02$, $\mathcal{G}_L^{tu\mu\mu} = V_{tb}V_{td}^*(-2 \pm 6) \sim 0.1$ [23].

We illustrate the strategy for a test of LU in the top sector but note that the ingredients are analogous to the ones in charm, Sect. 3.2. Let us assume, for concreteness, that dimuons provide the best measurement of the cross section $\sigma_{\mu\mu}$ in single top plus opposite sign same flavor leptons. It is induced by both left-handed and right-handed tops, $\sigma_{\mu\mu} = \kappa \sum_q \left(|\mathcal{K}_L^{tq\mu\mu}|^2 + |\mathcal{K}_R^{tq\mu\mu}|^2\right) + \bar{\sigma}_{\mu\mu}$, with proportionality constant κ. We can use this expression to obtain from a measurement of $\sigma_{\mu\mu}$ an upper limit on $|\mathcal{K}_R^{tq\mu\mu}|$; a stronger one would arise if the cross section induced by right-handed lepton contributions, $\bar{\sigma}_{\mu\mu} \propto |\mathcal{G}_L^{tq\ell\ell'}|^2 + |\mathcal{G}_R^{tq\ell\ell'}|^2$, could be determined and subtracted, or B-physics constraints on $|\mathcal{K}_L^{tq\mu\mu}|$ are imposed (see Tables 6, 7). However, the most conservative bound is obtained for $|\mathcal{K}_R^{tq\mu\mu}|$ saturating $\sigma_{\mu\mu}$. Assuming LU, the single top plus dineutrinos cross section reads, using (2),

$$\sigma_{\nu\nu}^{\text{LU}} = 3\kappa \left(\sum_{q=d,s} |\mathcal{K}_L^{bq\mu\mu}|^2 + \sum_{q=u,c} |\mathcal{K}_R^{tq\mu\mu}|^2 \right) , \tag{42}$$

hence

$$\sigma_{\nu\nu}^{\text{LU}} \leq 3 \left(\sigma_{\mu\mu} + \kappa \sum_{q=d,s} |\mathcal{K}_L^{bq\mu\mu}|^2 \right) , \tag{43}$$

and $\mathcal{K}_L^{bq\mu\mu}$ is bounded by the global $b \to s$ and $b \to d$ fits, with results given in Tables 4 and 5. To arrive at the simple expression (43) we assumed kinematic cuts for dileptons and dineutrinos to be identical. A violation of (43) indicates breakdown of lepton universality. Correspondingly, tests of cLFV are obtained as

$$\sigma_{\nu\nu}^{\text{cLFC}} = \kappa \sum_{\ell=e,\mu,\tau} \left(\sum_{q=d,s} |\mathcal{K}_L^{bq\ell\ell}|^2 + \sum_{q=u,c} |\mathcal{K}_R^{tq\ell\ell}|^2 \right) , \tag{44}$$

hence

$$\sigma_{\nu\nu}^{\text{cLFC}} \leq \sum_{\ell=e,\mu,\tau} \left(\sigma_{\ell\ell} + \kappa \sum_{q=d,s} |\mathcal{K}_L^{bq\ell\ell}|^2 \right) . \tag{45}$$

The expressions (43), (45) are schematic only as SM contributions have not been taken into account. A full collider analysis is beyond the scope of this paper. Note also that SM contributions from $Z \to \ell^+\ell^-$ could be controlled by cuts on the dilepon invariant mass, a feature that is not possible in $Z \to \nu\bar{\nu}$, hampering dineutrino searches at the LHC.

A bound on lepton-flavor specific $qt\ell\ell$ operators from $\ell^+\ell^-$ annihilating into $t\bar{q}$ at a future lepton collider can be obtained. The diagram for this process is shown in Fig. 4.

$$\sigma(\ell^+\ell^- \to t\bar{q}) = \frac{G_F^2\,\alpha_e^2}{(4\pi)^3}\, s\, f(\xi) \left(|\mathcal{K}_L^{tq\ell\ell}|^2 + |\mathcal{K}_R^{tq\ell\ell}|^2 \right) + \bar{\sigma} \tag{46}$$

where $f(\xi) = \xi^2\left(1 - \frac{1}{3}\xi\right)$ with $\xi = 1 - \frac{m_t^2}{s}$, and $\bar{\sigma}$ denotes contributions from $SU(2)_L$-singlet leptons. In polarized $\ell^+\ell^-$ collisions, the latter could be extracted.

We summarize strategies with single tops: Single top data in association with charged, opposite sign dileptons can be used to obtain quantitative predictions for single tops with dineutrinos assuming LU, or cLFC. Comparison to requisite, actual measurements of single tops with dineutrinos, as in (43), (45), allows to test the lepton flavor structure. The cLFC test requires data on dielectron, dimuon and ditau spectra, whereas the LU test can be performed using dimuons, or more general, a single species' cross section, alone. Irrespective of concrete studies with single tops associated with charged dileptons, the tests can be performed using input on the SMEFT coefficients from elsewhere, as in (42), (44). Presently, the right-hand sides are dominated by the poorly constrained couplings with right-handed tops, $\mathcal{K}_R^{tq\ell\ell}$. LHC sensitivities in single top production with dileptons [28] are encouraging and suggest that the 3000 fb^{-1} HL-LHC can probe couplings at the level of $|\mathcal{K}_R^{tc\mu\mu}| \lesssim 22$ and $|\mathcal{K}_R^{tu\mu\mu}| \lesssim 2.2$. A dedicated analysis of missing energy collider distributions, *i.e,* computing κ as a function of kinematic cuts and efficiencies, would be desirable but is beyond the scope of this study.

5 Summary

Thanks to the flavor-inclusiveness of missing energy measurements at particle physics experiments, $SU(2)_L$-links of neutrinos with the charged leptons (2) allow to probe lepton flavor structure in dineutrino observables in three benchmarks: charged lepton flavor violation, charged lepton flavor conservation and lepton universality. We put forward concrete, novel tests in charm, beauty and top, exploiting the connection between the up- and the down-sector. Tests invoke experimental findings from the charged lepton sector and will evolve with them in the future.

Key predictions for rare charm decays are upper limits on the dineutrino branching ratios corresponding to the benchmarks universality, lepton flavor conservation and including

charged LFV, compiled in Table 3. The missing energy modes are well-suited for the experiments Belle II [24], BES III [32], and future e^+e^--colliders, such as an FCC-ee running at the Z [29] or the super-tau-charm factory (STCF) [33], with sizable charm rates. Since any observation of $c \to u\,\nu\bar{\nu}$ transitions heralds NP, experimental analysis is encouraged.

Interestingly, despite the lack of constraints from top FCNCs, the beauty sector allows to test lepton universality using dineutrino decays, thanks to correlations between B-decay modes involving different final state hadrons, notably $B \to K\nu\bar{\nu}$ versus $B \to K^*\nu\bar{\nu}$, and $B \to \pi\nu\bar{\nu}$ versus $B \to \rho\nu\bar{\nu}$, see Sect. 4.1. Corresponding tests are suitable for Belle II and a Z-factory.

Analyses testing lepton flavor structure with rare top decays, discussed in Sect. 4.3, are similar to rare charm decays: a negligible SM background together with constraints on NP from the down-sector. In addition to FCNC top decays, rare top couplings from semileptonic four-fermion operators can be probed in single top plus dileptons – to be compared to single top plus missing energy, see Sect. 4.4. While a dedicated sensitivity study is beyond the scope of this work we note that studies with ditops and dileptons including $tq\ell\ell$ in the signal simulation are already available from the LHC [27]. Improving limits on such couplings is key to improve lepton flavor-symmetry predictions for $|\Delta t| = |\Delta(u, c)| = 1$ dineutrino channels (38).

We conclude that processes with dineutrinos offer new and model-independent ways to test the SM and its approximate flavor symmetries, and to shed light on the persistent hints for universality violation in B-decays, e.g., [34].

We close by commenting on the effects of light, right-handed neutrinos, not covered by the SMEFT framework, on the tests of lepton flavor structure [13,22]. The presence of both SM-like and right-handed neutrinos allows for pseudo (-scalar) four-fermion operators, that induce decays of mesons annihilating to dineutrinos. Quantitatively, improving the bound $\mathcal{B}(D^0 \to \nu\bar{\nu}) < 9.4 \cdot 10^{-5}$ at 90 % CL [21] by about 2 orders of magnitude would suppress theses effects to be within the theoretical uncertainty in the $|\Delta c| = |\Delta u| = 1$ studies reported here. Improving $\mathcal{B}(B_d^0 \to \nu\bar{\nu}) < 2.4 \cdot 10^{-5}$ at 90 % CL [18] down to $5 \cdot 10^{-7}$ would suffice for the pseudo (-scalar) contribution to be at most percent level in semileptonic $|\Delta b| = |\Delta d| = 1$ decays. Presently no bound on $B_s^0 \to$ invisibles exists but one at the level of Belle II projections, $\mathcal{B}(B_s^0 \to \nu\bar{\nu}) < 1.1 \cdot 10^{-5}$ with $0.5\,\text{ab}^{-1}$ [24],would allow for similar control of the impact of right-handed neutrinos in $|\Delta b| = |\Delta s| = 1$ decays.

Note added: A very recent search by BES III reports $\mathcal{B}(D^0 \to \pi^0\nu\bar{\nu}) < 2.1 \cdot 10^{-4}$ at 90% CL [35], which is about one order of magnitude away from being constraining, see Table 3.

Acknowledgements This work is supported by the *Studienstiftung des Deutschen Volkes* (MG) and the *Bundesministerium für Bildung und Forschung* – BMBF (HG).

Data Availability Statement This manuscript has no associated data or the data will not be deposited. [Authors' comment: There are no data because this is theoretical work.]

Funded by SCOAP[3].

References

1. Y. Grossman, Z. Ligeti, E. Nardi, Nucl. Phys. B **465**, 369–398 (1996) https://doi.org/10.1016/0550-3213(96)00051-X. https://arxiv.org/abs/hep-ph/9510378 (Erratum: Nucl. Phys. B 480, 753–754 (1996))
2. G. Hiller, APS Phys. **7**, 102 (2014)
3. G. Ciezarek, M. Franco Sevilla, B. Hamilton, R. Kowalewski, T. Kuhr, V. Lüth, Y. Sato, Nature **546**, 227–233 (2017). https://arxiv.org/abs/1703.01766 [hep-ex]
4. G. Eilam, J.L. Hewett, A. Soni, Phys. Rev. D **44**, 1473-1484 (1991). https://doi.org/10.1103/PhysRevD.44.1473 (**Erratum: Phys. Rev. D 59, 039901 (1999)**)
5. G. Burdman, E. Golowich, J.L. Hewett, S. Pakvasa, Phys. Rev. D **66**, 014009 (2002). https://arxiv.org/abs/hep-ph/0112235
6. Y. Grossman, G. Isidori, H. Murayama, Phys. Lett. B **588**, 74–80 (2004). https://arxiv.org/abs/hep-ph/0311353
7. A.J. Buras, J. Girrbach-Noe, C. Niehoff, D.M. Straub, JHEP **02**, 184 (2015). https://arxiv.org/abs/1409.4557 [hep-ph]
8. B. Grzadkowski, M. Iskrzynski, M. Misiak, J. Rosiek, JHEP **10**, 085 (2010). https://arxiv.org/abs/1008.4884 [hep-ph]
9. A. Efrati, A. Falkowski, Y. Soreq, JHEP **07**, 018 (2015). https://arxiv.org/abs/1503.07872 [hep-ph]
10. I. Brivio, S. Bruggisser, F. Maltoni, R. Moutafis, T. Plehn, E. Vryonidou, S. Westhoff, C. Zhang, JHEP **02**, 131 (2020). https://arxiv.org/abs/1910.03606 [hep-ph]
11. R. Alonso, E.E. Jenkins, A.V. Manohar, M. Trott, JHEP **04**, 159 (2014). https://arxiv.org/abs/1312.2014 [hep-ph]
12. F. Feruglio, P. Paradisi, A. Pattori, JHEP **09**, 061 (2017). https://doi.org/10.1007/JHEP09(2017)061. https://arxiv.org/abs/1705.00929 [hep-ph]
13. R. Bause, H. Gisbert, M. Golz, G. Hiller, JHEP **12**, 061 (2021). https://doi.org/10.1007/JHEP12(2021)061. https://arxiv.org/abs/2109.01675 [hep-ph]
14. J. Fuentes-Martin, A. Greljo, J. Martin Camalich, J.D. Ruiz-Alvarez, JHEP **11**, 080 (2020). https://arxiv.org/abs/2003.12421 [hep-ph]
15. A. Angelescu, D.A. Faroughy, O. Sumensari, Eur. Phys. J. C **80**(7), 641 (2020). https://arxiv.org/abs/2002.05684 [hep-ph]

16. R. Mandal, A. Pich, JHEP **1912**, 089 (2019). https://doi.org/10.1007/JHEP12(2019)089. https://arxiv.org/abs/1908.11155 [hep-ph]
17. J. Brod, M. Gorbahn, E. Stamou, PoS **BEAUTY2020**, 056 (2021). https://doi.org/10.22323/1.391.0056. https://arxiv.org/abs/2105.02868 [hep-ph]
18. P.A. Zyla et al. [Particle Data Group], PTEP **2020**(8), 083C01 (2020). https://doi.org/10.1093/ptep/ptaa104
19. R. Bause, M. Golz, G. Hiller, A. Tayduganov, Eur. Phys. J. C **80**(1), 65 (2020). https://arxiv.org/abs/1909.11108 [hep-ph] (**Erratum: Eur. Phys. J. C 81 (2021) no.3, 219**)
20. H. Gisbert, M. Golz, D.S. Mitzel, Mod. Phys. Lett. A **36**(04), 2130002 (2021). https://arxiv.org/abs/2011.09478 [hep-ph]
21. Y.-T. Lai et al. [Belle Collaboration], Phys. Rev. D **95**(1), 011102 (2017). https://arxiv.org/abs/1611.09455 [hep-ex]
22. R. Bause, H. Gisbert, M. Golz, G. Hiller, Phys. Rev. D **103**(1), 015033 (2021). https://arxiv.org/abs/2010.02225 [hep-ph]
23. R. Bause, H. Gisbert, M. Golz, G. Hiller, Model-independent analysis of $b \to d$ processes. DO-TH 21-30 (**In preparation**)
24. E. Kou et al. [Belle-II Collaboration]. PTEP **2019**(12), 123C01 (2019). https://arxiv.org/abs/1808.10567 [hep-ex]
25. [CMS], Search for charged lepton flavor violation in top quark production and decay in proton–proton collisions at $\sqrt{s} = 13$ TeV. CMS-PAS-TOP-19-006
26. [ATLAS], Search for charged lepton-flavour violation in top-quark decays at the LHC with the ATLAS detector. ATLAS-CONF-2018-044
27. A.M. Sirunyan et al. [CMS], JHEP **03**, 095 (2021). https://doi.org/10.1007/JHEP03(2021)095. https://arxiv.org/abs/2012.04120 [hep-ex]
28. Y. Afik, S. Bar-Shalom, A. Soni, J. Wudka, Phys. Rev. D **103**(7), 075031 (2021). https://doi.org/10.1103/PhysRevD.103.075031. https://arxiv.org/abs/2101.05286 [hep-ph]
29. A. Abada et al. [FCC Collaboration], Eur. Phys. J. C **79**(6), 474 (2019)
30. J.P. Delahaye, M. Diemoz, K. Long, B. Mansoulié, N. Pastrone, L. Rivkin, D. Schulte, A. Skrinsky, A. Wulzer, https://arxiv.org/abs/1901.06150 [physics.acc-ph]
31. F. Zimmermann, https://doi.org/10.18429/JACoW-IPAC2018-MOPMF065
32. M. Ablikim et al., Chin. Phys. C **44**(4), 040001 (2020). https://arxiv.org/abs/1912.05983 [hep-ex]
33. A.E. Bondar et al., [Charm-Tau Factory]. Phys. Atom. Nucl. **76**, 1072–1085 (2013). https://doi.org/10.1134/S1063778813090032
34. S. Bifani, S. Descotes-Genon, A. Romero Vidal, M.H. Schune, J. Phys. G **46**(2), 023001 (2019). https://arxiv.org/abs/1809.06229 [hep-ex]
35. M. Ablikim et al. [BESIII], https://arxiv.org/abs/2112.14236 [hep-ex]